American Mineralogist, Volume 65, pages 1150–1165, 1980

The influence of TiO_2 on the structure and derivative properties of silicate melts

BJØRN O. MYSEN

Geophysical Laboratory, Carnegie Institution of Washington
Washington, D. C. 20008

FREDERICK J. RYERSON

Department of Terrestrial Magnetism, Carnegie Institution of Washington
Washington, D. C. 20015

AND DAVID VIRGO

Geophysical Laboratory, Carnegie Institution of Washington
Washington, D. C. 20008

Abstract

The influence of TiO_2 on the structure of silicate melts has been determined at 1 atm pressure by laser Raman spectroscopy. The following melt compositions were used: $CaSiO_3$, $CaMgSi_2O_6$, Na_2SiO_3, $NaAlSi_3O_8$, $CaAl_2O_8$, and Na_2TiO_3.

Titanium is in four-fold coordination in all melts studied, as there are no Raman bands below 700 cm^{-1} that can be assigned to Ti^{4+} in six-fold coordination. In melts with nonbridging oxygen (NBO), solution of TiO_2 results in a decrease in NBO/T (nonbridging oxygens per tetrahedrally coordinated cation). In metasilicate melts, monomers, chains, and sheets of Si^{4+} and Ti^{4+} occur as discrete units. The proportion of the Ti-rich structural units increases relative to the Si-rich units with increasing TiO_2 content of the system. The overall NBO/T of the melt decreases with increasing TiO_2 content which results in an increase of chain and sheet units relative to monomers.

Titanium substitutes for silicon in quenched Ab and An melts to form three-dimensional (3*D*) aluminotitanate complexes. The aluminosilicate complexes (3*D*) in these melts become depleted in Al as a result of this solution mechanism of Ti. Discrete, three-dimensional units of TiO_2 composition occur together with three-dimensional SiO_2 units in quenched melts in the system SiO_2–TiO_2.

The position of liquidus boundaries between minerals of different degree of polymerization shifts toward the silica-deficient portions of the appropriate systems with the addition of TiO_2. This behavior is a result of the decrease in NBO/T in the melts as TiO_2 is added.

Crystal–liquid partition coefficients for a variety of transition metals and incompatible trace elements are likely to increase with increasing TiO_2 content of the melt as a result of the decrease of NBO/T of melts with increasing TiO_2 content.

The viscosity of depolymerized silicate melts depends on NBO/T. Inasmuch as this ratio decreases with increasing TiO_2, the viscosity of such melts probably increases with increasing titanium content. The viscosity of fully polymerized melts depends on the strength of Al–O–Si and Si–O–Si bonds. By substitution of Ti for some of the Si, the bonds probably become weaker. The viscosity of such melts will decrease, therefore, with increasing TiO_2 content.

Introduction

Titanium is a minor element in most rock-forming silicate melts. Nevertheless, this element is petrologically significant. For example, liquidus boundaries between olivine and pyroxene shift toward olivine-rich portions of appropriate systems as TiO_2 is added to the melt (Kushiro, 1973, 1974, 1975).

Titanium also plays an important role in Fe–Ti oxides when such minerals are used to determine $f(O_2)$–T conditions during the petrogenesis of ig-

0003–004X/80/1112–1150$02.00

neous rocks (Buddington and Lindsley, 1964; Carmichael, 1967). The composition of an Fe–Ti oxide depends on the activity of Fe^{2+}, Fe^{3+}, and Ti^{4+} in the igneous system. Consequently, it is necessary to understand the structural role of Ti^{4+}, Fe^{3+}, and Fe^{2+} in the silicate melts from which such minerals precipitate. Some data are already available for ferric and ferrous iron (Waff, 1977; Mysen and Virgo, 1978; Mysen *et al.*, 1979a; Seifert *et al.*, 1979); however, little is known about Ti^{4+}.

Crystal–liquid partition coefficients of important trace elements (*e.g.*, transition metals and rare earth elements) depend on the extent of polymerization of silicate melts (Hart and Davis, 1978; Watson, 1976; Mysen *et al.*, 1979b). The extent of this polymerization depends on the Ti content of the melt and whether Ti exists in four-fold or six-fold coordination. It is important, however, to determine the role of Ti before the influence of dissolved TiO_2 on trace-element partition coefficients can be understood.

The physical properties of silicate melts such as viscosity and compressibility probably vary with Ti content. These variables depend on both the degree of polymerization and the strength of oxygen bridges in the silicate melts (Bridgman and Simon, 1953; Bockris *et al.*, 1955; Taylor and Rindone, 1970; Mysen *et al.*, 1979a; Bottinga and Weill, 1972).

In view of these observations, we have conducted a Raman spectroscopic study of selected Ti-bearing silicate melts, in order to determine the structure of possible Ti-bearing complexes and to assess the interaction between such complexes and the silicate solvent.

Experimental technique

Igneous rocks are made up essentially of a combination of components that when studied independently in a molten state consist of a three-dimensional network (*e.g.*, feldspars and quartz) or have two or more nonbridging oxygens per tetrahedral cation (NBO/T). The latter group involves all the pyroxene compositions, for example. We decided, therefore, to study the influence of TiO_2 on the structures of these two groups of melts.

Pure SiO_2–TiO_2 melts have been studied by Chandrasekhar *et al.* (1979) and Tobin and Baak (1968). Their data serve as reference points for the structural studies of feldspar compositions [$NaAlSi_3O_8$ (Ab) and $CaAl_2Si_2O_8$ (An)]. Three metasilicate compositions were used: Na_2SiO_3 (NS), $CaSiO_3$ (Wo), and $CaMgSi_2O_6$ (Di). In addition, the spectrum of quenched melt of Na_2TiO_3 composition was taken to aid in assigning the Ti–O stretching band in Ti-bearing structural units having a significant number of nonbridging oxygens.

The starting materials were spectroscopically pure SiO_2, Al_2O_3, TiO_2, MgO, and $CaCO_3$, and reagent-grade Na_2CO_3. These oxides were thoroughly mixed, melted, and quenched in a platinum-wound vertical quench furnace. The samples were quenched by dripping droplets of melts on a Pt surface cooled with liquid N_2. The quenching rate with this technique was about 500°C/sec over the first 1000°C.

Inasmuch as analyses of Na-rich glasses tend to be unreliable (see, for example, discussion by Mysen and Virgo, 1978), sample compositions were checked with the aid of Raman spectroscopy as discussed in detail by Mysen *et al.* (1980a). That method provides information on both sample composition and sample homogeneity.

All aspects of the Raman spectroscopic technique have been discussed by Mysen *et al.* (1980b), who also discussed procedures for deconvolution of the Raman spectra. Further details of that procedure as it pertains to the Ti-bearing samples are discussed below.

Results

Metasilicate compositions

Raman spectra of Ti-free, quenched melts of Wo, Di, and NS composition have been discussed elsewhere (Brawer and White, 1975, 1977; Mysen *et al.*, 1979a, 1980b; Seifert *et al.*, 1979; Furukawa and White, 1980), and only the high-frequency envelopes of these spectra are shown here (Figs. 1–3). Detailed spectroscopic data are shown in Table 1. The Raman spectra of quenched melts on MO–SiO_2 and M_2O–SiO_2 joins (M = Pb^{2+}, Ca^{2+}, Mg^{2+}, K^+, and Na^+) in the compositional range between orthosilicate (NBO/Si = 4) and tectosilicate (NBO/Si = 0) were discussed by Mysen *et al.* (1980b) and Virgo *et al.* (1980), who pointed out that only a limited number of anionic structural units occur in these melts. These are of the form SiO_4^{4-}, $Si_2O_7^{6-}$, $Si_2O_6^{4-}$, $Si_2O_5^{2-}$, and SiO_2. Only three of these units could coexist for a given melt compositional range. Within each range the proportion, but not the composition, of the units varied as a function of bulk composition of the melt. Among other tetrahedrally coordinated cations, only Al^{3+} appears to mix randomly with Si^{4+}.

The model is inconsistent with melt structural models based on polymer theory (*e.g.*, Masson, 1977). Mysen *et al.* (1980b) discussed the differences

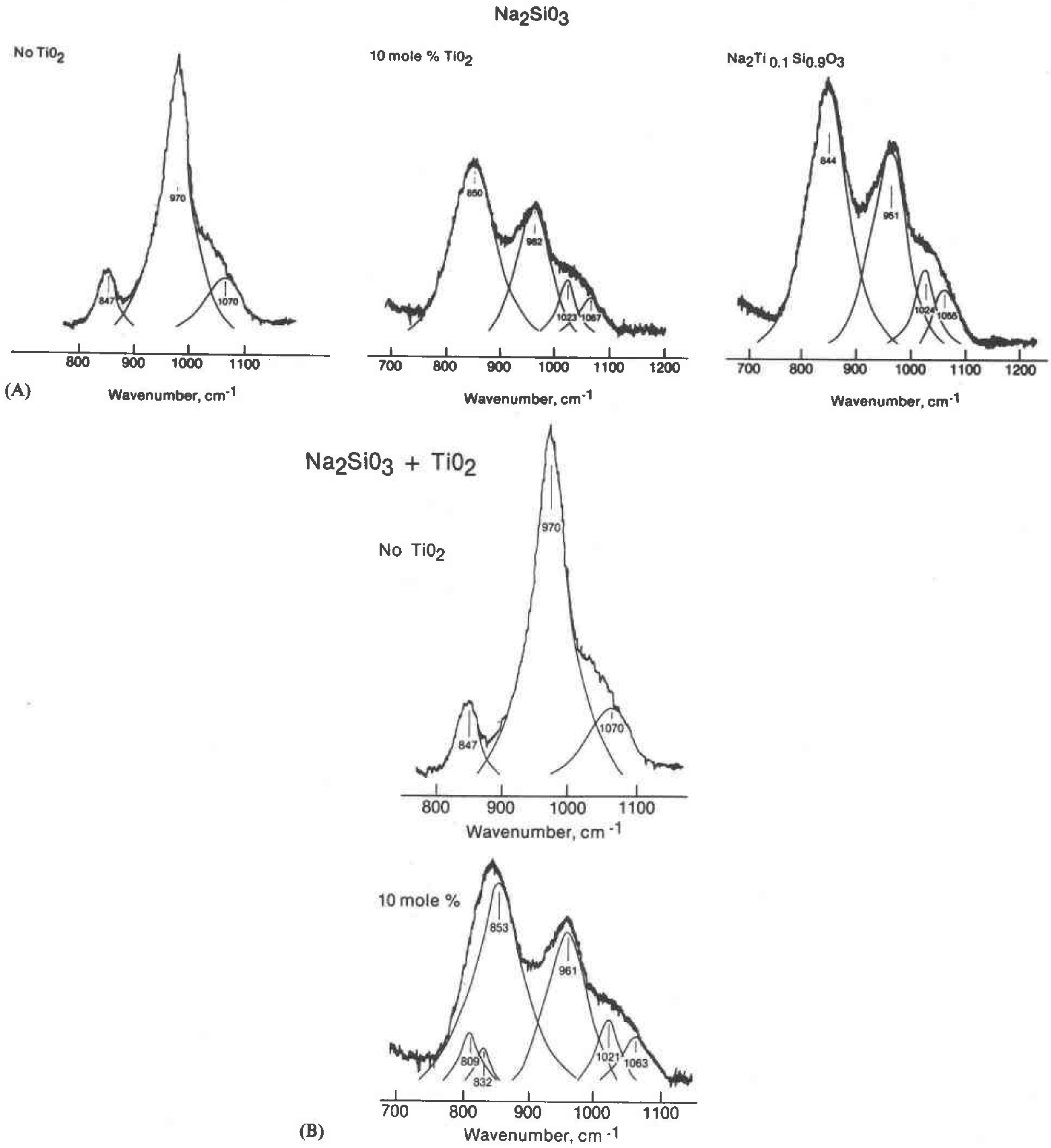

Fig. 1. Two alternative interpretations of the high-frequency envelope of the unpolarized Raman spectrum of quenched Na_2SiO_3 melts as a function of TiO_2 content. (A) One-band fit in the 880 cm^{-1} maximum. (B) Three-band fit in the 880 cm^{-1} maximum. See text for discussion of deconvolutions.

and pointed out that their simple model was consistent not only with the Raman spectroscopic data, but also with crystal chemical principles (*e.g.*, Dent Glasser, 1979) and rheological properties of the melts. Models based on polymer theory are not.

The model proposed by Mysen *et al.* (1980b) is the basis for this work. As they discussed the Raman spectra and the interpreted structures of metasilicates in detail, only a summary of those data and discussion is included here.

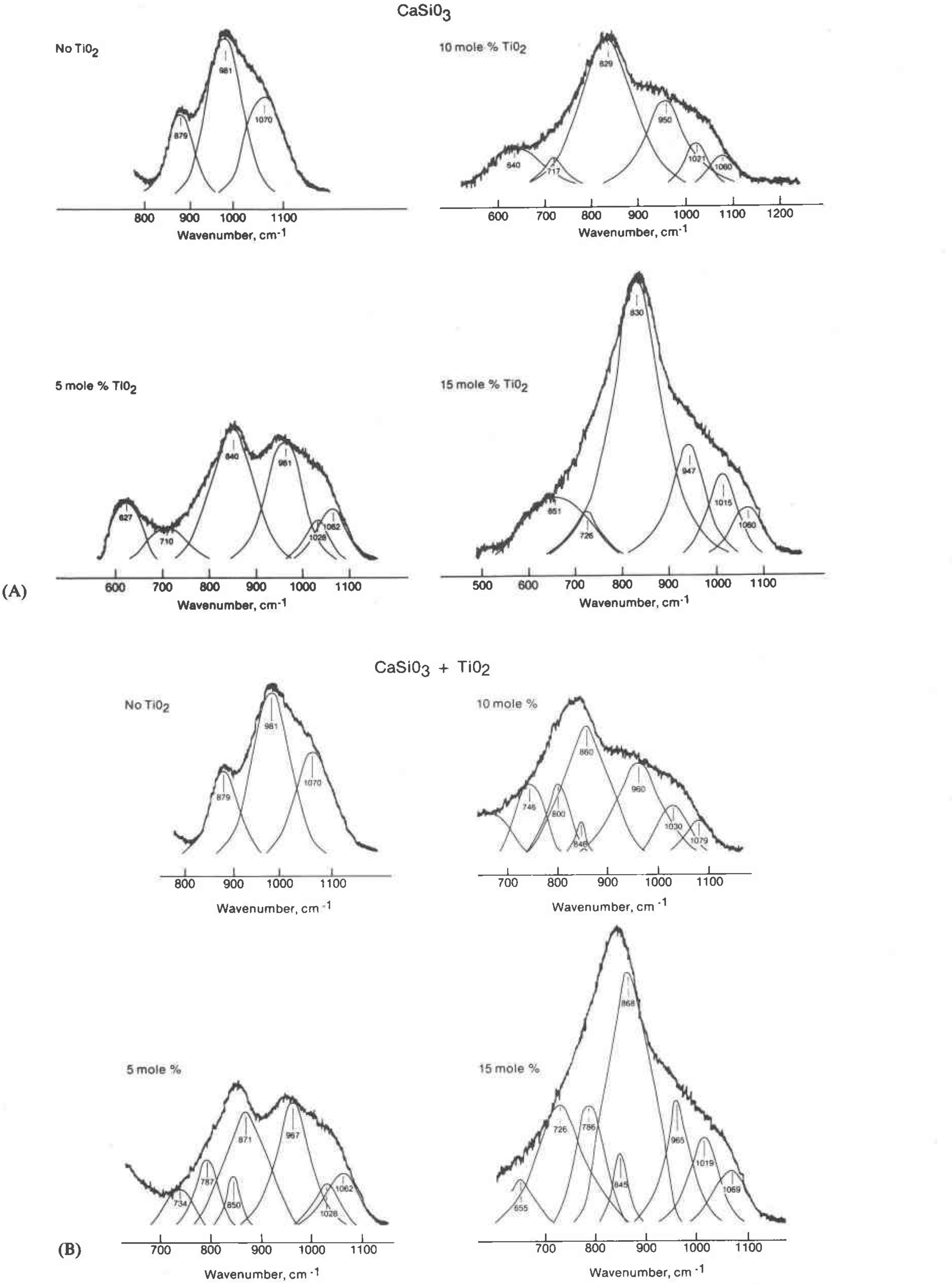

Fig. 2. Two alternative interpretations of the high-frequency envelope of the unpolarized Raman spectrum of quenched $CaSiO_3$ melts as a function of TiO_2 content. A and B as in Fig. 1. See text for discussion of deconvolutions.

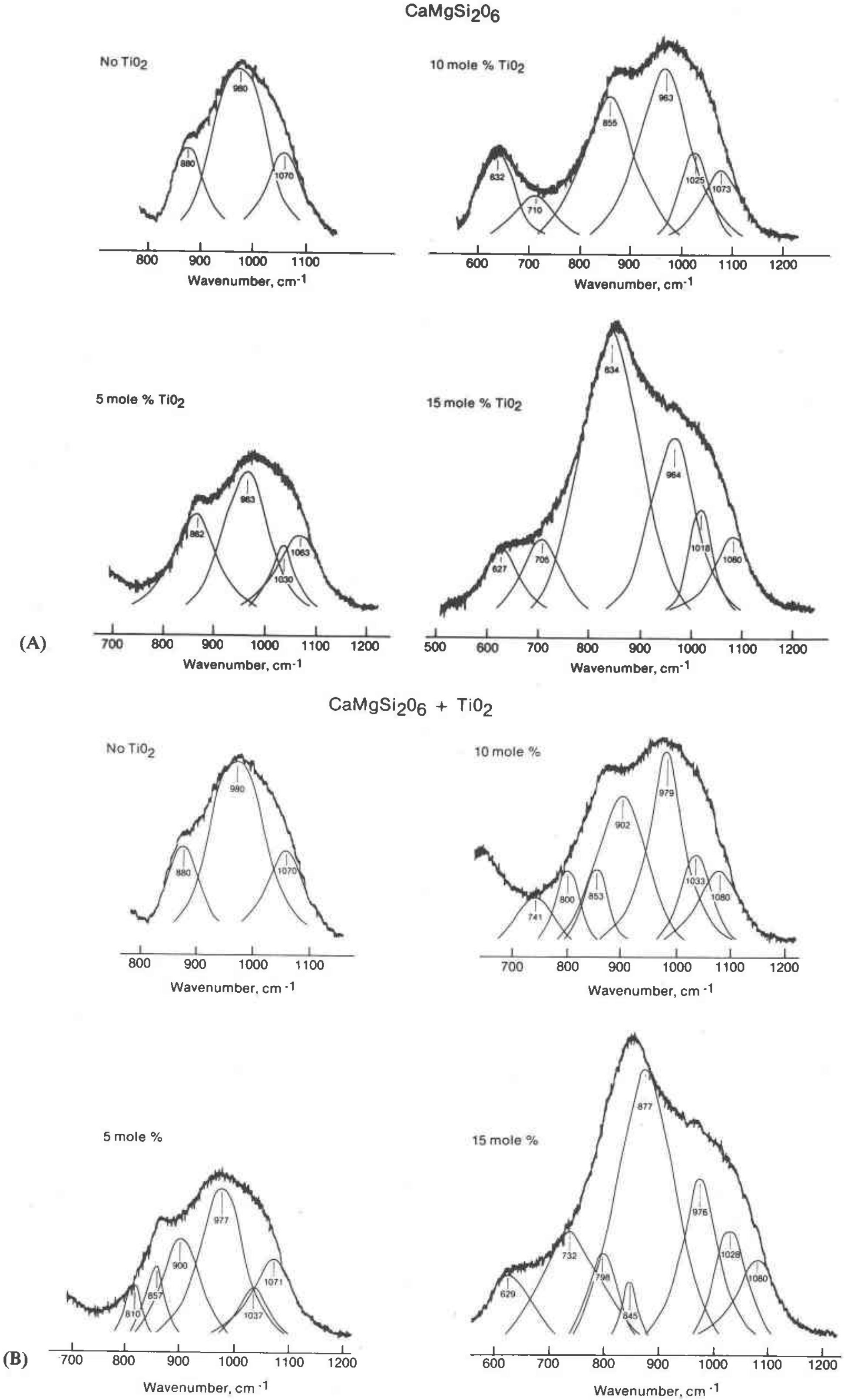

Fig. 3. Two alternative interpretations of the high-frequency envelope of the unpolarized Raman spectrum of quenched $CaMgSi_2O_6$ melts as a function of TiO_2 content. A and B as in Fig. 1.

Table 1. Raman data on depolymerized melts with TiO_2

Composition	Temp., °C	Wavenumber, cm^{-1}									
$CaSiO_3$	1575	...	...	637s	...	...	879m	...	979s	...	1070s
$CaSiO_3$ + 5 mole % TiO_2	1575	[345m(bd)	...	627s	710mw	...	840s	...	961s	1028mw	1062m]
		345m(bd)	...	627s	734w	787m	850w	871s	967s	1028w	1062mw
$CaSiO_3$ + 10 mole % TiO_2	1575	[340m(bd)	...	640mw	717m	...	829s	...	950m	1021mw	1060w]
		340m(bd)	...	640mw	746m	800m	846w	860s	960s	1030m	1079w
$CaSiO_3$ + 15 mole % TiO_2	1575	[310m(bd)	500vw	651m	726mw	...	830s	...	947m	1015m	1060m]
		310m(bd)	500vw	655m	726m	786m	845w	868s	965m	1019m	1069mw
$CaMgSi_2O_6$	1575	...	...	632s	...	...	880m	...	983s	...	1070m
$CaMgSi_2O_6$ + 5 mole % TiO_2		[350vw(bd)	...	638m	...	...	862s	...	963s	1030mw	1063m]
		350vw(bd)	...	638m	...	810w	857m	900ms	977s	1037w	1071m
$CaMgSi_2O_6$ + 10 mole % TiO_2	1575	[330w(bd)	510vw	632m	710w	...	855s	...	963s	1025m	1073m]
		330w(bd)	510vw	632m	741w	800m	853s	902s	979s	1033m	1080m
$CaMgSi_2O_6$ + 15 mole % TiO_2	1575	[315mw(bd)	520w	627m	705m	...	834s	...	964s	1018m	1080m]
		315mw(bd)	520w	629m	732m	798m	845w	877s	976ms	1028m	1080m
Na_2SiO_3	1400	...	...	620s	...	...	860m	...	970s	...	1056m
Na_2SiO_3 + 10 mole % TiO_2	1400	[350w(bd)	500vw	618m	...	...	850m	...	962s	1023mw	1067w(bd)]
$Na_2Ti_{0.1}Si_{0.9}O_3$	1400	[350w(bd)	500vw	614m	...	...	844s	...	951s	1024mw	1066w]

Abbreviations: s, strong; ms, medium to strong; m, medium; mw, medium to weak; w, weak; vw, very weak; (bd), broad; (sh), shoulder. Band positions in brackets are those from interpretation A (only one band fitted to the 880 cm^{-1} maximum in the high-frequency envelope of the spectra).

The high-frequency envelope of the Raman spectrum of Ti-free, quenched Wo melt consists of three major bands. These are a symmetric $Si–O^{2-}$ stretch band near 880 cm^{-1}, a symmetric $^-O–Si–O^-$ stretch band near 980 cm^{-1}, and a symmetric $^-O–Si–O^0$ stretch band near 1070 cm^{-1}. The notations for the stretch bands (introduced by Furukawa and White, 1980), are meant to imply structural units with 4, 2, and 1 NBO/Si, respectively. The 980 and 1070 cm^{-1} stretch bands are also associated with O–Si–O deformation motions in the frequency region between 600 and 660 cm^{-1} (Table 1; see also Etchepare, 1972; Lazarev, 1972).

As a part of their comprehensive model for silicate melt structure, Mysen *et al.* (1980b) concluded that the structure of metasilicate melts consists of units with, on the average, 4, 2, and 1 NBO/Si. These units are referred to as monomers, chains, and sheets in the following text. The exact nature of these structural units was also discussed by Mysen *et al.* (1980b), who concluded that these structures are, most likely, monomers, chains, and sheets.

The Raman spectra of quenched $CaMgSi_2O_6$ (Di) and $NaSiO_3$ (NS) melt (Table 1) consist of the same bands with the same relative intensities and polarization characteristics as $CaSiO_3$ (Wo) melt. Mysen *et al.* (1980b) concluded, therefore, that those melts contain the same anionic structural units as Wo melt.

Before the influence of TiO_2 on the Raman spectra of metasilicate quenched melts is considered, the spectrum of quenched Na_2TiO_3 melt will be discussed (Fig. 4). The high-frequency envelope of this spectrum indicates the presence of three bands. One is near 770 cm^{-1}, another is near 880 cm^{-1}, and there is a strong band near 270 cm^{-1}. The Raman spectra of quenched melts on the joins $Na_2O–TiO_2–SiO_2$, $Li_2O–TiO_2–SiO_2$, and $K_2O–TiO_2–SiO_2$ (Iwamoto *et al.*, 1975; Furukawa and White, 1979) exhibit the same bands for analogous compositions but with some Si^{4+} substituted for Ti^{4+}. Inasmuch as (Si,Ti)-systems exhibit two-mode behavior (see Furukawa and White, 1979, 1980), and there is no evidence of (Si,Ti)-coupling in the (Si,Ti)-bearing systems (Furukawa and White, 1979), the interpretation of the O–Ti–O vibrations in the Si-bearing systems is not affected by the presence of Si^{4+} in the system.

Furukawa and White (1979) noted that in analogy with band positions in crystalline titanates with Ti^{4+} in six-fold coordination, the spectra of quenched melts on these joins do not indicate that Ti^{4+} is in six-fold coordination (Ti–O stretch bands below about 650 cm^{-1} for Ti^{VI}–O polyhedra). The absence of such low-frequency bands in the spectrum of quenched Na_2TiO_3 melt indicates that all Ti^{4+} is in four-fold coordination.

Furukawa and White (1979) suggested that the maximum near 880 cm^{-1} reflects a band that is characteristic of Ti^{4+} incorporated in a sheet structure

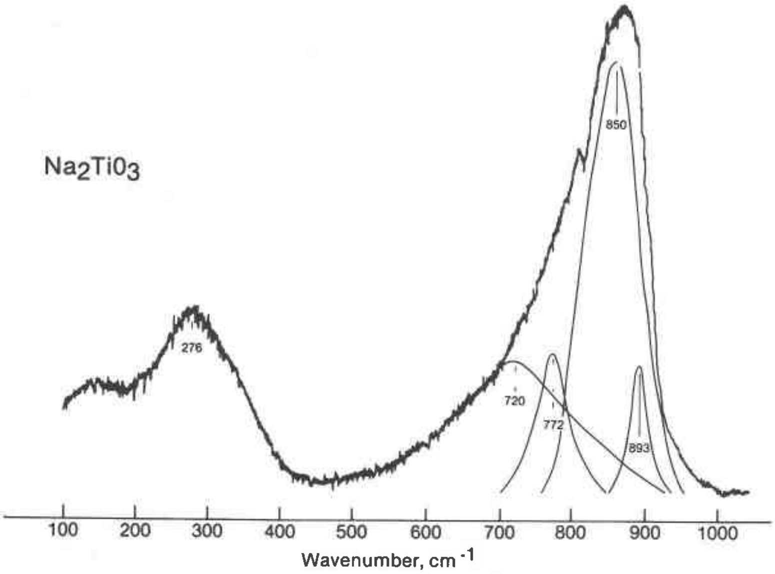

Fig. 4. Unpolarized Raman spectrum of quenched Na_2TiO_3 melt. See text for further discussion of the spectrum and deconvolution.

($^-$O–Ti–O^0 stretch vibration) in Ti-bearing Li-disilicate quenched melts. In the spectrum in Figure 4 the maximum of the high-frequency envelope is near 880 cm^{-1}, but the melt is a less polymerized metasilicate. By analogy with the spectroscopic results on melts on the join Na_2O–SiO_2 (Brawer and White, 1975; Furukawa and White, 1980; Mysen *et al.*, 1980b), a chain structure is probably the dominant structural unit in the metatitanate. Inasmuch as the frequencies of stretch vibrations are expected to decrease with increasing NBO/T (*e.g.*, Furukawa and White, 1979), it is unlikely that the maximum at 880 cm^{-1} reflects only one vibration, as 880 cm^{-1} corresponds to the $^-$O–Ti–O^0 (sheet). Furthermore, the high-frequency envelope shows a distinct asymmetry toward lower frequencies. If the main band in the maximum near 880 cm^{-1} is placed at a lower frequency, another band at higher frequency is required to equalize the area beneath the high-frequency envelope. This band is near 890 cm^{-1}. We suggest that this band is due to the $^-$O–Ti–O^0 stretch vibration observed by Furukawa and White (1979) in Li-disilicate with TiO_2. The main band is near 850 cm^{-1} and probably reflects the presence of $Ti_2O_6^{4-}$ chain units in the melt. Mass-balance considerations indicate that a metatitanate with sheet and chain units in the structure must have at least one structural unit with NBO/T greater than that of a chain (2). The Ti–O stretch band of crystalline orthotitanates with Ti^{4+} in four-fold coordination occurs near 750 cm^{-1}. The Raman spectrum of pure Na_2TiO_3 quenched melt is best fitted with a sharp band near 770 cm^{-1} and a broad band near 720 cm^{-1}. We suggest that the 770 cm^{-1} band results from a Ti–O stretch vibration from the depolymerized unit. This unit may be a monomer, although the spectroscopic data do not provide an unambiguous answer. If it is a monomer, quenched Na_2TiO_3 melt displays the same structural units as Na_2SiO_3 melt (Mysen *et al.*, 1980b); that is, there are a sheet, a chain, and monomer and the chain unit is the predominant unit in the melt.

In the structural model proposed for Na_2TiO_3 melt, structural units contain bridging oxygen. Bands reflecting O–Ti–O deformation might be expected. We suggest that the 720 cm^{-1} band is such a band.

Furukawa and White (1979, 1980) found that the addition of GeO_2 and TiO_2 to melts on M_2O–SiO_2 joins resulted in a "two-mode behavior," in which for each Si–O stretch band there is an analogous Ge–O or Ti–O stretch band. Similar observations were made by Mysen *et al.* (1979a, 1980a) and Seifert *et al.* (1979), as a result of the addition of Fe_2O_3 to melts of similar composition. If this observation holds true for the present systems as well, the Raman spectra of Ti-bearing, silicate systems should show one band for the Si–O stretch vibration and one for the analogous Ti–O vibration. The Raman spectrum of quenched melt of Na_2SiO_3 + 10 mole percent TiO_2 (O = 6) is compared with that of Ti-free quenched NS melt in Figure 1 (see also Table 1). The high-frequency envelope of the spectrum is marked by two strong maxima near 850 and 950 cm^{-1}. There is also a shoulder extending to about 1100 cm^{-1}. If one band is fitted near 1070 cm^{-1} [this band occurs in the Ti-free sample and results from $^-$O–Si–O^0 stretching in a sheet structure (Furukawa and White, 1980)] and one in a maximum near 960 cm^{-1} [corresponding to $^-$O–Si–O$^-$ stretching in a chain structure (Brawer and White, 1975, 1977; Furukawa and White, 1980)] another band must be fitted near 1020 cm^{-1}. Not only do the 1070 and 960 cm^{-1} bands have the same frequencies as the sheet and chain stretch bands in Ti-free melt, but they also have the same polarization characteristics (see also Furukawa and White, 1980). The band near 1020 cm^{-1} probably results from (Si,Ti) coupling of stretch vibrations in a sheet unit with randomly distributed Ti^{4+} and Si^{4+}. Such mixing is needed to explain this band, because $^-$O–Ti–O^0 stretching results in a band near 890 cm^{-1} (see above) and $^-$O–Si–O^0 stretching results in a band near 1070 cm^{-1}. An intermediate band position may indicate mixing of the two.

The maximum near 850 cm^{-1} presents a problem (Fig. 1). A single band can be fitted to the maximum (Fig. 1A), and the band would be interpreted as due to $^-$O–Ti–O$^-$ stretching ($Ti_2O_6^{4-}$ chain). In such a case, Ti-bearing quenched NS melt has a structure that consists almost entirely of $Ti_2O_6^{4-}$ and $Si_2O_6^{4-}$ chains, a sheet unit that is essentially $Si_2O_5^{2-}$, and a sheet unit of mixed Ti and Si [$(Si,Ti)_2O_5^{2-}$]. The individual units would be at least 20Å across, inasmuch as separate Raman bands can be assigned to these units (Brawer, 1975). In all other systems studied to date, at least three structural units with different degrees of polymerization (different NBO/T) occur together in binary and more complex systems (Virgo *et al.*, 1979). Chain and sheet structures could coexist with either three-dimensional units (3*D*) or a monomer. In the system Na_2O–SiO_2 the 3*D* unit does not occur until molar $2 < SiO_2/Na_2O < 3$ (Mysen *et al.*, 1980b). There is no clear antisymmetric indication from the Raman spectrum that stretch bands indicative of three-dimensional structural units occur (Fig. 1). If TiO_2 is considered analogous to SiO_2, these three-dimensional network units would not be expected in quenched NS + 10 mole percent TiO_2 melt. Insertion of a new stretch band at frequencies below 850 cm^{-1} was therefore attempted. The (Ti,Si) coupling would not be expected in monomers, and Raman bands from Si–O^{2-} and Ti–O^{2-} stretch vibrations are expected to be rather sharp. Sharp bands are expected because there is no bridging oxygen where the dihedral angle may vary, and broadening of the Raman bands will occur (Brawer, 1975). The results of the above considerations are shown in Figure 1B. There is a strong band at 853 cm^{-1} and two weak bands near 830 and 810 cm^{-1}. We suggest that the latter two bands may reflect Si–O^{2-} and Ti–O^{2-} stretching, respectively. According to this interpretation, Ti-bearing quenched melt of Na_2SiO_3 composition exhibits the same two-mode behavior as found in NS melt with Fe_2O_3 added (Mysen *et al.*, 1979a). Under such circumstances, the melt consists of two monomer units (TiO_4^{4-} and SiO_4^{4-}), two types of chain units ($Si_2O_6^{4-}$ and $Ti_2O_6^{4-}$), and two sheet units [$Si_2O_5^{2-}$ and $(Si,Ti)_2O_5^{2-}$]. The size of the units cannot be determined. According to the theory of Brawer (1975), decoupling of Raman bands may occur if the individual units are of the order of 20Å or greater. We conclude, therefore, that each of these units is at least that large.

The high-frequency envelopes of the Raman spectra of quenched Wo melt with 5–15 mole percent TiO_2 are shown in Figure 2 (see also Table 1) with two alternative deconvolutions of the spectra. As for quenched NS melt, the Raman spectra alone cannot be used to determine which solution is correct, and both will be discussed. The three highest frequency bands occur at nearly the same position in both solutions (Fig. 2A,B). The band near 1060 cm^{-1} occurs whether or not TiO_2 is present, and in analogy with previous interpretations (Furukawa and White, 1979, 1980; Mysen *et al.*, 1979a, 1980b) it is assigned to $^-$O–Si–O^0 stretching. The frequency of this band is insignificantly affected by the presence of TiO_2. Consequently, the sheet unit that gives rise to this band must be nearly Ti-free. The band between 1020 and 1030 cm^{-1} shifts to slightly lower frequency and grows in intensity relative to the 1060 cm^{-1} band as the TiO_2 content of quenched Wo melt is increased (Figs. 5 and 6). This band is therefore related to the presence of Ti^{4+} in the melt. In analogy with the interpretation of the same band in quenched NS + 10 mole percent TiO_2 melt, the band is assigned to $^-$O–(Si,Ti)–O^0 symmetric stretching. A consequence of this logic and the Raman spectroscopic features (Figs. 5 and 6) is that this structural unit becomes more Ti-rich as the Ti content of the system increases.

The band between 980 and 950 cm^{-1} (Fig. 2) shifts to slightly lower frequency with increasing Ti content (Fig. 5). The intensity of this band also decreases relative to the other bands in the envelope as the Ti content of the system increases. This band may be due to stretching of the (Si,Ti)-coupled stretch band in a chain unit. The frequency is near that of the $^-$O–

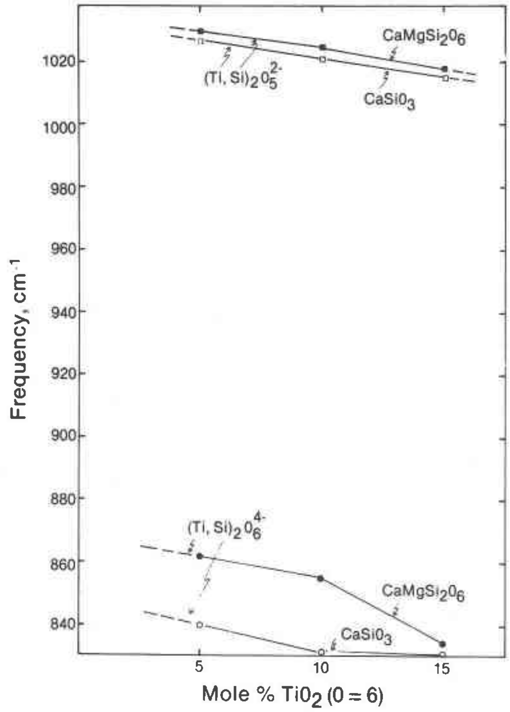

Fig. 5. Frequency shifts of important Raman bands according to interpretation A in Fig. 1–3.

$Si–O^-$ stretch band in the Ti-free system, and the Ti content of the structural units must be low. Its frequency shift with increasing Ti content may indicate, however, a slight increase in its Ti content with increasing TiO_2 in the system.

The main spectroscopic feature of the spectra of quenched Wo + TiO_2 melt is the maximum between 830 and 840 cm^{-1}. This maximum becomes more dominant and shifts to slightly lower frequency with increasing Ti content (Fig. 2; see also Table 1). When only one band is fitted to this maximum (Fig. 2A), the band occurs at about 30 cm^{-1} lower frequency than the band considered diagnostic of a pure $Ti_2O_6^{4-}$ chain unit on the basis of the data from quenched Na_2TiO_3 melt (Figs. 2A and 4). If this is the only band in the region near 830 cm^{-1}, and does in fact reflect the presence of a Ti-rich chain unit in the melt, the spectroscopic evidence indicates that the $Ti_2O_6^{4-}$ chain unit becomes the dominant structural feature of quenched Wo melt as the Ti content of the system is increased (Fig. 6). The downward frequency shift with increasing Ti content also indicates that there is some Si in the chain and that the Ti/(Ti + Si) increases with increasing Ti content.

No spectroscopic evidence indicates that Ti^{4+} is in six-fold coordination in quenched Wo + TiO_2 melt, inasmuch as there are no bands at wavenumbers less than ~700 cm^{-1} that could be attributed to Ti–O stretch vibrations of Ti in six-fold coordination. The band near 650 cm^{-1} is the second most intense band in all metasilicate melts (Brawer and White, 1975,

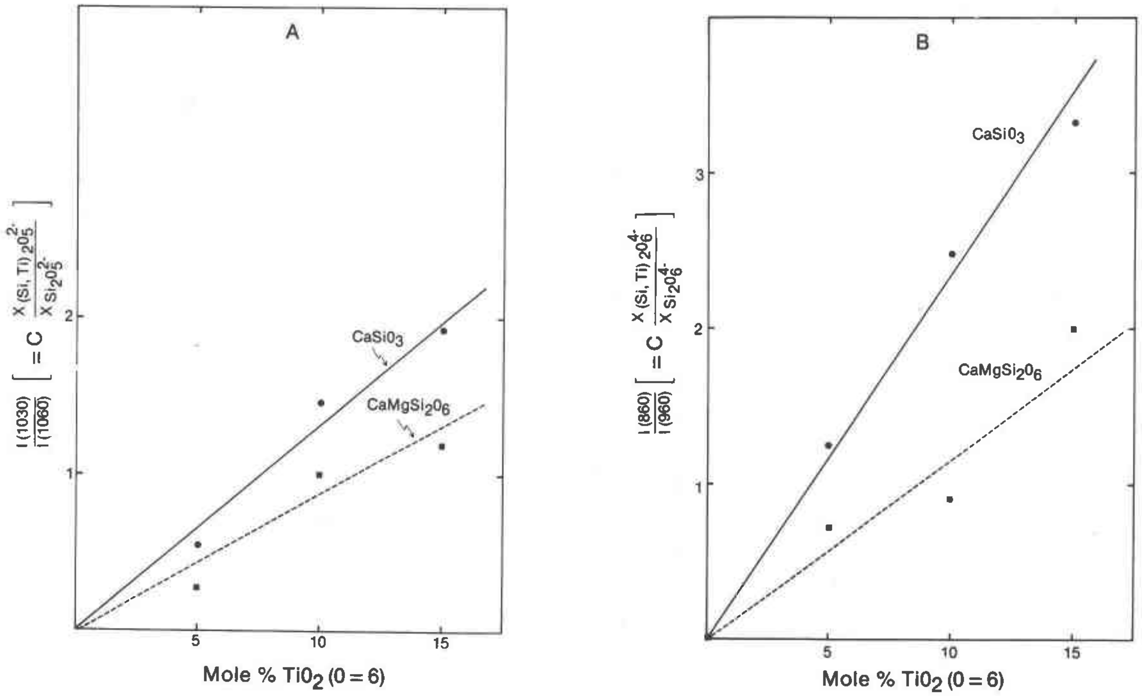

Fig. 6. Variations of intensity ratios indicating relative importance of Ti-rich and Ti-depleted structural units in quenched metasilicate melts according to interpretation A in Fig. 1–3.

1977; Furukawa and White, 1980; Verweij, 1979a,b; see also Mysen *et al.*, 1980b, for summary and discussion of data for binary-metal oxide–silica melts) and is interpreted as an O–Si–O deformation motion (see also above). Its frequency and intensity relative to the high-frequency envelope are not affected by the presence of TiO_2 in the melt. We conclude, therefore, that no new bands (which indicate six-fold coordinated Ti^{4+}) occur in this frequency region as TiO_2 is added. Rather, it appears that Ti^{4+} is a network-former whose role in the melts is similar to that of Si^{4+}.

Virgo *et al.* (1980) have shown that up to 25 mole percent SiO_2 may be added to Wo melt without stabilization of new structural units. The proportion of the other units in the melt is, however, affected by this process. It is not likely, therefore, that addition of up to 15 mole percent TiO_2 would result in the disappearance of the monomer in the structure. Furthermore, the absence of any indication in the spectra of a 3*D* unit suggests that Ti^{4+} is no more effective than Si^{4+} in producing a decrease of NBO/T of the melt. In view of the above discussion of the structure of quenched NS + 10 mole percent TiO_2, the existence of Raman bands indicating the presence of structural units with NBO/T greater than 2 was searched for. The strongest Raman band near 850 cm^{-1} was placed as close as possible to that of the Ti–O stretch band of a $Ti_2O_6^{4-}$ chain unit (see Figs. 4 and 2B). As a result of this procedure, there is no room for additional bands between the 960 cm^{-1} band and that near 850 cm^{-1}. The symmetric Si–O stretch band for a dimer ($Si_2O_7^{6-}$) occurs near 900 cm^{-1} (Lazarev, 1972; Virgo *et al.*, 1980; Mysen *et al.*, 1980b). Stretch bands from structural units with NBO/T < 3.5 occur at even higher frequencies. We conclude, therefore, the Ti-free structural units with 3.5 > NBO/T > 2 do not exist in quenched Wo + TiO_2 melt. An attempt was then made to fit a band near the position of the $Si–O^{2-}$ stretch band found in Ti-free Wo melt (Fig. 2). If such a band is fitted to the high-frequency envelope, another sharp band occurs near 800 cm^{-1} and a broad one is developed near 720 cm^{-1}. The sharpness of the 850 cm^{-1} band indicative of a depolymerized structural unit is justified, as for the bands in the same position in quenched NS + 10 mole percent TiO_2 discussed above. From spectroscopic considerations, it cannot be ruled out that both the 850 and 800 cm^{-1} bands thus generated reflect (Si,Ti)-coupled vibrations in structural units with 4 > NBO/T > 2. Note, however, that in the systems CaO–SiO_2 and (Ca,Mg)O–SiO_2, such units occur only when molar $MO/TO_2 \geq$ 1.2. In the present system, molar MO/TO_2 is less than 1. Note also that in the simple system CaO–SiO_2, monomers exist in melts with as much as 25 mole percent SiO_2 added to $CaSiO_3$ (MO/SiO_2 = 0.67). We suggest, therefore, that the two bands near 850 and 800 cm^{-1} are $Si–O^{2-}$ and $Ti–O^{2-}$ stretch bands. The band in the vicinity of 720 cm^{-1} probably is due to O–Ti–O or O–(Si,Ti)–O deformation in chain or sheet units or both.

The spectroscopic interpretation shown in Figure 2B is similar to that for NS + TiO_2 melt in Figure 1B. This interpretation is also consistent with other work in analogous systems (*e.g.*, summary by Virgo *et al.*, 1979, 1980) and indicates a two-mode behavior in the system Wo + TiO_2. Such behavior was also found by Furukawa and White (1979) in the system Li_2O–TiO_2–SiO_2, by Furukawa and White (1980) in the system Na_2O–GeO_2–SiO_2, and by Seifert *et al.* (1979) in the system Na_2O–Al_2O_3–FeO–Fe_2O_3–SiO_2.

The intensity ratios, *I*(800)/*I*(850) and *I*(870)/*I*(970), reflect the abundance ratios $X(TiO_4^{4-})/X(SiO_4^{4-})$ and $X(Ti_2O_6^{4-})/X(Si_2O_6^{4-})$ in the melt. The data in Figure 7 show that the $Ti_2O_6^{4-}$ chain increases in abundance relative to the $Si_2O_6^{4-}$ chain to at least 15 mole percent TiO_2. The abundance of TiO_4^{4-} monomers relative to SiO_4^{4-} monomers passes through a maximum near 10 mole percent TiO_2. The intensity ratio, *I*(1030)/*I*(1060) (Fig. 7), indicates that the relative abundances of the sheet units change in the same fashion as those of the monomers. Note, however, that the titaniferous sheet unit also contains Si and that Ti/(Ti + Si) increases as the bulk TiO_2 content of the system increases beyond 10 mole percent (Fig. 2). It cannot be determined from the spectra how the bulk monomer/chain/sheet ratios vary as a function of TiO_2 content, because of the different polarizability of Ti–O and analogous Si–O bonds.

The high-frequency envelopes of the Raman spectra from quenched TiO_2-bearing melt of $CaMgSi_2O_6$ composition (Di) are shown in Figure 3 with the same alternative interpretations as for quenched NS + TiO_2 (Fig. 1) and quenched Wo + TiO_2 (Fig. 2). The evolution of the spectra with increasing TiO_2 content resembles that of quenched Wo melt with TiO_2 (Figs. 2 and 3).

As for the two previous compositions, the spectra without additional bands below about 850 cm^{-1} are discussed first (Fig. 3A). Note that all bands grow in intensity and shift frequencies in the same fashion as in Wo + TiO_2 (Figs. 2, 3, 5–7). The interpretations therefore are similar.

The Raman spectra of quenched melts on the join

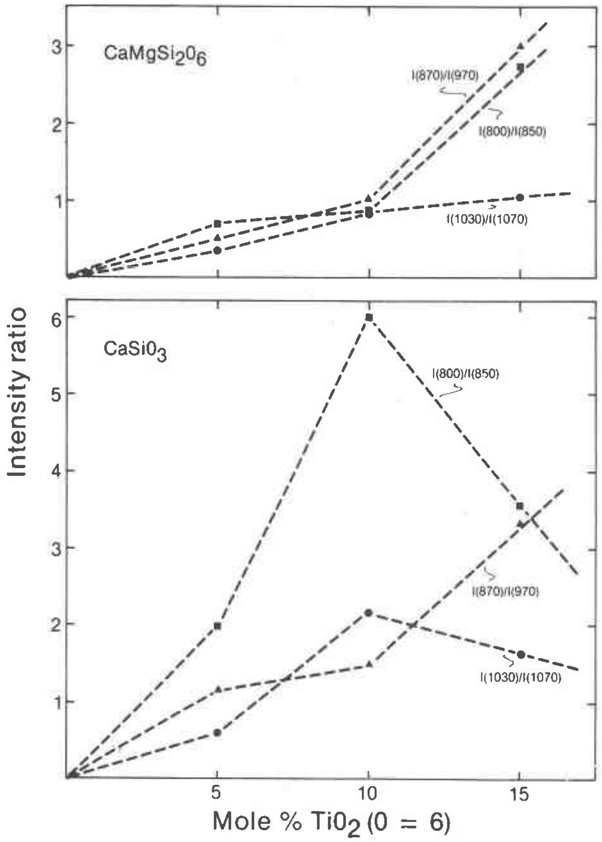

Fig. 7. Variations of intensity ratios of critical Raman bands according to interpretation B in Fig. 2 and 3. See text for further discussion.

$(Ca_{0.5}Mg_{0.5})O$–SiO_2 indicate that more than 25 mole percent SiO_2 must be added to Di melt to form melts with structures that involve three-dimensional network units (Virgo *et al.*, 1980; Mysen *et al.*, 1980b). With SiO_2 contents less than 25 mole percent, the quenched melts contain sheets, chains, and monomers. With this conclusion as a guide, curves were fitted to the high-frequency envelope so that bands from stretch vibrations in polymeric units with NBO/T greater than 2 could be included (Fig. 3B). The results are similar to those for Wo + TiO_2 (Fig. 2B). Note, however, that in contrast to the results for Wo + TiO_2, the intensity ratios, *I*(800)/*I*(850), *I*(870)/*I*(970), and *I*(1030)/*I*(1060), increase continuously to at least 15 mole percent TiO_2 (Fig. 7). It appears that *I*(1030)/*I*(1060) is the least sensitive to TiO_2 content.

As indicated above, it cannot be decided from the Raman spectra alone whether models A or B are correct. However, in view of the conclusion that Ti^{4+} shows a two-mode behavior in all other systems considered (Furukawa and White, 1980), and because of the otherwise similar behavior of Ti^{4+} and Si^{4+}, we suggest that model B is more likely. If so, we conclude that addition of TiO_2 to metasilicate melts has the same structural effect whether the metal is Na, Ca, or Mg. That is, it appears that in addition to the silicate monomers, chains, and sheets, the analogous titanate complexes are formed. Only the sheet unit consists of a mixture of Si^{4+} and Ti^{4+}. The size of these units cannot be determined. According to Brawer (1975), the existence of separate bands indicates that they are at least 20Å across.

Three-dimensional network structures

Raman spectra of quenched melts in the system SiO_2–TiO_2 have been published by Tobin and Baak (1968) and Chandrasekhar *et al.* (1979). In the high-frequency region between 800 and 1200 cm^{-1}, two Si–O^0 stretch bands at 1060 and 1190 cm^{-1} [indicative of two three-dimensional structural units, as also supported by transmission electron microscopy; Gaskell (1975), Bando and Ishizuka (1979), Gaskell and Mistry (1979)] have been joined by two Ti–O^0 stretch bands near 930 and 1100 cm^{-1}. The frequency of these two bands is independent of the TiO_2 content of the melt (Chandrasekhar *et al.*, 1979), indicating that these two bands are decoupled from the Si–O^0 stretch vibrations. Chandrasekhar *et al.* suggested that the presence of the 930 and 1100 cm^{-1} bands in quenched melts in the system SiO_2–TiO_2 reflected *LO* and *TO* splitting. Inasmuch as such splitting requires long-range order, a condition that does not exist in glasses and melts, this interpretation is not likely. Rather, we suggest that two separate TiO_2 units exist in the melt, in analogy with the SiO_2 units whose presence is further supported by independent transmission electron microscopic data (Gaskell, 1975; Bando and Ishizuka, 1979; Gaskell and Mistry, 1979). This interpretation was also advanced by Virgo *et al.* (1979) for melts on the joins $NaAlO_2$–SiO_2, $CaAl_2O_4$–SiO_2, and $NaFeO_2$–SiO_2. In this case, the interpretation was further substantiated by the observation that the extent of splitting of the two bands diminished with increasing content of the aluminate (or ferrite) component. If the presence of the two stretch bands were due to *LO* and *TO* splitting, increased splitting would be expected.

We suggest, therefore, that in addition to the two discrete three-dimensional SiO_2 units, two TiO_2 units with a three-dimensional structure also exist in these melts. These observations will be used as a guide to determine the structural role of Ti^{4+} in quenched melts of Ab and An composition.

Five and ten mole percent TiO_2 were added to Ab melt. The high-frequency envelope of the Raman spectra of these quenched melts is compared with the high-frequency envelope of TiO_2-free, quenched Ab melt (Fig. 8; see also Table 2). The anionic structure of TiO_2-free, quenched Ab melt has been described previously (Virgo *et al.,* 1979). The two most important bands are those at 991 and 1095 cm^{-1}, reflecting (Si,Al)–O^0 stretching derived from two distinct three-dimensional network units. Virgo *et al.* (1979) and Mysen *et al.* (1980b) noted that the highest frequency band is more sensitive to changes in $Si/(Si + Al)$ than the lowest frequency, antisymmetric stretch band indicative of the three-dimensional structure of $NaAlSi_3O_8$ melt. Similar observations were made in the systems $CaAl_2O_4$–SiO_2, $NaFeO_2$–SiO_2 and $NaGaO_2$–SiO_2. On this basis and on the basis that the molar extinction coefficients of these vibrations are likely to be similar, they concluded that the highest frequency band was more Al-rich than the lowest frequency band.

The addition of TiO_2 to Ab melt results in two new bands near 900 and 1050 cm^{-1}. The intensity of these two new bands increases with increasing TiO_2 content of the quenched melt. The two original (Si,Al)–O^0 stretch bands have shifted to slightly higher frequency as a result of the dissolved TiO_2, and the intensity ratio, $I(1000)/I(1100)$, has increased (Fig. 8). The increase in frequency of the two (Si,Al)–O^0 stretch bands indicates that the three-dimensional structural units responsible for the existence of these two bands have become less aluminous as the TiO_2 content of the aluminosilicate melt is increased. The increase of $I(1000)/I(1100)$ indicates that the proportion of the most aluminous, three-dimensional network units has decreased at the expense of the more Si-rich unit.

The two Ti–O^0 stretch bands occur at somewhat lower frequency in quenched Ab + TiO_2 melt (Fig. 8) than in quenched SiO_2 + TiO_2 melt (Chandrasekhar *et al.,* 1979). This reduction in frequency indicates that the Ti–O^0 vibrations are coupled with either Al or Si. In view of the diminished importance of Al in the (Si,Al) portion of the network when TiO_2 is added, the two bands near 1050 and 900 cm^{-1} are probably (Ti,Al)–O^0 stretch vibrations.

In view of the above considerations, we conclude that in melts in the system $NaAlSi_3O_8$–TiO_2 only three-dimensional network structures exist. The networks consist of two discrete (Si,Al)-bearing three-dimensional units and two discrete (Ti,Al)-bearing three-dimensional units.

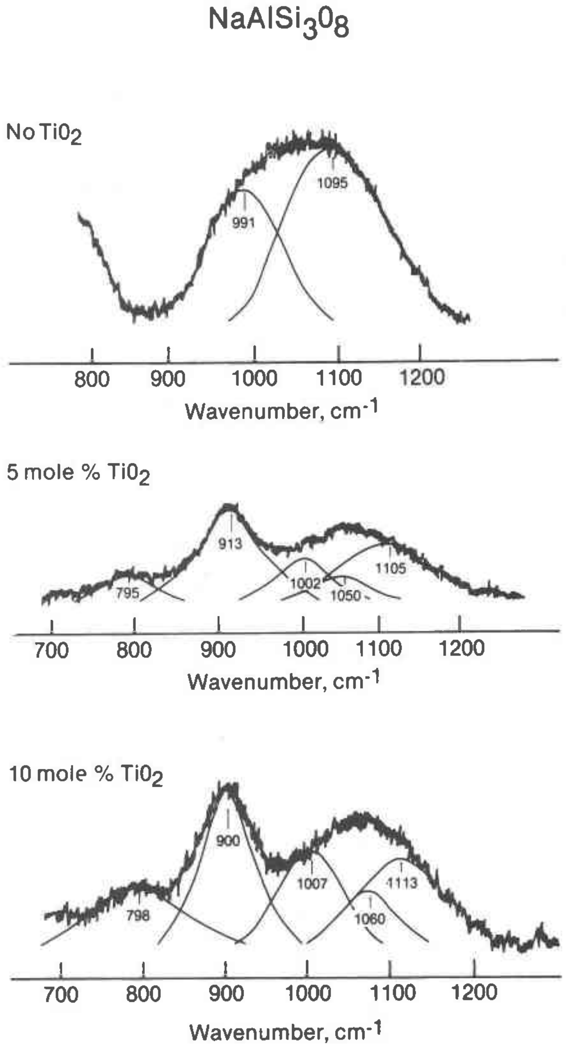

Fig. 8. High-frequency envelope of unpolarized Raman spectrum of quenched melt of $NaAlSi_3O_8$ composition as a function of TiO_2 content.

Five and ten mole percent TiO_2 were also added to melt of An composition. The resulting Raman spectra are shown in Figure 9 (see also Table 2) and compared with that of a Ti-free sample. The Raman spectra of quenched Ti-bearing An melt resemble those of quenched Ti-bearing Ab melt (Figs. 8 and 9). There are two new bands in the high-frequency region as a result of added TiO_2 (at 860–900 cm^{-1} and 1070–1080 cm^{-1}). Furthermore, with 10 mole percent TiO_2 added, the highest frequency (Si,Al)–O^0 stretch band (at 1000 cm^{-1}) is shifted to 1084 cm^{-1}. In addition, the intensity ratio of the original 950–1000 cm^{-1} bands has increased, as also observed for quenched melts in the system ($NaAlSi_3O_8$ + TiO_2 (Fig. 8).

Table 2. Raman data on quenched melts on the join $NaAlSi_3O_8$–$CaAl_2Si_2O_8$–TiO_2

Composition	Temp., °C	Wavenumber, cm^{-1}						
$NaAlSi_3O_8$	1575	470s	566w	780(sh)	...	991s	...	1095s
$NaAlSi_3O_8$ + 5 mole % TiO_2	1575	446s	577w	795w(bd)	913s	1002m	1050w(bd)	1105s
$NaAlSi_3O_8$ + 10 mole % TiO_2	1575	453s	583w	798m(bd)	900s	1007m	1060w	1113m
$CaAl_2Si_2O_8$	1575	500s	574w	750vw(bd)	...	950m(bd)	...	1000s
$CaAl_2Si_2O_8$ + 5 mole % TiO_2	1575	494s	570vw	800vw(bd)	900m	950s	1007s	1073m
$CaAl_2Si_2O_8$ + 10 mole % TiO_2	1575	481s	574vw	795w(bd)	862s	922s	998s	1084w

Symbols as in Table 1.

It may be argued that the band near 1000 cm^{-1} with as much as 10 mole percent TiO_2 in solution is, in fact, one of the (Si,Al)-coupled stretch bands. This conclusion is unlikely, however, because (1) its intensity increases with increasing Ti content relative to the rest of the high-frequency envelope and (2) the frequency of the 900 cm^{-1} Ti–O^0 stretch band shifts to even lower values with increasing Ti content, indicating that this is a coupled vibration. The 950 cm^{-1} band [(Si,Al)–O^0 stretch] also shifts to lower frequency with increasing Ti content. We suggest, therefore, that solution of TiO_2 in melt of An composition results in the formation of two (Ti,Al)-bearing three-dimensional network units. The most Al-rich, (Si,Al)-coupled, three-dimensional structural unit has become considerably enriched in Si relative to Al.

Melts vs. quenched melts

In this study, quenched melts have been used to determine the structure of molten silicates. In order to relate the structural information from quenched melts to structural features of silicate melts, it is necessary to document that the structural features under consideration are not significantly affected by quenching. Riebling (1968) and Taylor *et al.* (1980) found that the anionic units (silicate polymers) in melts with a three-dimensional network structure, such as melts of $NaAlSi_3O_8$ composition, remain the same as the melt is quenched to a glass. Direct experimental proof of structural similarity between melts and their quenched analogues on the join Na_2O–SiO_2 was provided by Sweet and White (1969) and Sharma *et al.* (1978). In those studies, infrared and Raman spectra of melts of $Na_2Si_3O_7$, $Na_2Si_2O_5$, and Na_2SiO_3 composition were compared with those of their glasses. It was concluded that the structures of these melts and glasses were similar in the sense that there were no discernible differences between the spectra of the two forms of the compositions.

On the basis of the above information, we conclude that the structural features of silicate melts that can be determined with Raman spectroscopy are quenchable. The results given in this report are applicable, therefore, to molten silicates.

Solubility mechanisms

The spectroscopic data indicate that Ti^{4+} is in fourfold coordination in all the melts studied and that Ti^{4+} makes the same structural units as Si^{4+}. The existence of distinct bands that stem from Ti-bearing complexes rather than coupled (Si,Ti) bands indicates that discrete titanate complexes occur rather than random (Si,Ti) substitution.

Before addressing the role of TiO_2 in metasilicate melts, a short summary of the equilibria describing the structure of metasilicate melts is necessary. Virgo *et al.* (1980) and Mysen *et al.* (1980b) summarized all available spectroscopic data and combined these data with other properties, leading to the conclusion that the anionic structure of metasilicate melts may be described with the expression:

$$3Si_2O^{4-} \text{ (chain)} = 2SiO_4^{4-} \text{ (monomer)} + 2Si_2O_5^{2-} \text{ (sheet)} \qquad (1)$$

Solution of TiO_2 in silicate melts with NBO/T > O results in additional tetrahedral polyhedra with a concomitant reduction of NBO/T. Monomers are probably present in all melts. Chains and sheets also occur. Consequently an expression analogous to equation 1 applies:

$$3T_2O_6^{4-} \text{ (chain)} = 2TO_4^{4-} \text{ (monomer)} + 2T_2O_5^{2-} \text{ (sheet)} \qquad (2)$$

The presence of discrete titanate complexes in melts with NBO/T > 0 is suggested by the Raman

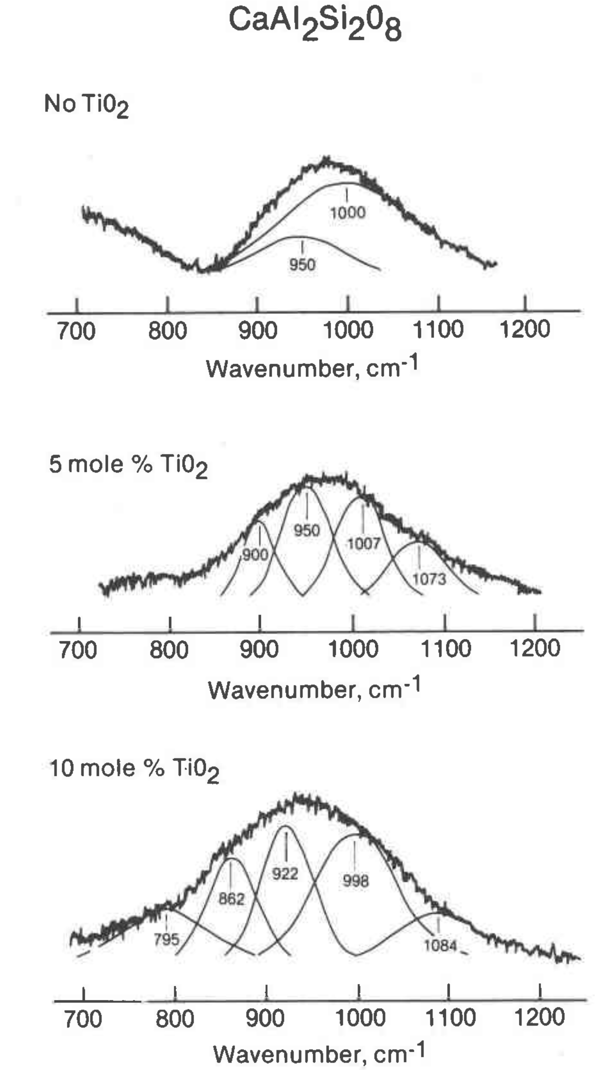

Fig. 9. High-frequency envelope of unpolarized Raman spectra of quenched melt of $CaAl_2Si_2O_8$ composition as a function of TiO_2 content.

spectroscopic data. In order to maintain local charge balance, these titanate complexes must compete with silicate complexes to coordinate metal cations. This competition is represented by the following reaction:

$$\text{Si–O–M–O–Si} + \text{Ti–O–Ti} = \text{Si–O–Si} + \text{Ti–O–M–O–Ti} \qquad (3)$$

where M represents the metal cation. Hence, the addition of TiO_2 to basic silicate melts causes some portion of the nonbridging oxygens in the silicate melts to be transformed to bridging oxygen, thereby polymerizing this portion of the silicate network. This mechanism is analogous to that proposed by Mysen and Virgo (1979) and Ryerson and Hess (1979) for solution of CO_2 and P_2O_5, respectively, in basic melts, and helps explain the diminished importance of monomers in TiO_2-bearing metasilicate melts.

Published Raman data on the system SiO_2–TiO_2 (Tobin and Baak, 1968; Chandrasekhar *et al.,* 1979) indicate that three-dimensional discrete TiO_2 units are formed in the melt. These units do not seem to have any Si^{4+}. In aluminosilicate melts with a three-dimensional network structure, the data indicate that more complex aluminotitanate units are formed at the expense of the original aluminosilicate units, so that the latter units become less aluminous. The $NaAl_2O_2/TiO_2$ and $CaAl_2O_4/TiO_2$ in three-dimensional aluminum titanate complexes increase and $NaAlO_2/SiO_2$ and $CaAl_2O_4/SiO_2$ decrease in aluminum silicate complexes as the TiO_2 content of these melts increases. Again, there is no evidence for interaction with Si^{4+} in the titanium-bearing complexes. We propose, therefore, that the aluminum titanate and aluminum silicate units are random mixtures of three-dimensional $NaAlO_2$ and $CaAl_2O_4$ with TiO_2 to make $NaAlTi_3O_8$ and $CaAl_2Ti_2O_8$ complexes.

Applications

Kushiro (1975) noted that the presence of TiO_2 in melts near the join Mg_2SiO_4–SiO_2 results in a substantial shift of the forsterite–protoenstatite liquidus boundary toward the forsterite-rich portion of the system. In fact, protoenstatite melts congruently at 1 atm pressure with about 6 wt. percent TiO_2 present (corresponding to about 13 mole percent TiO_2 in $Mg_2Si_2O_6$). TiO_2 had a similar effect on the pseudowollastonite–cristobalite liquidus boundary (the boundary shifts toward the metasilicate portion of the system). Our data on the effects of TiO_2 on melt structures indicate that the equilibrium expressed with an equation like 1 is replaced by equation 2 or 3 where no monomers exist in the melt. Consequently, it would be expected that orthosilicate minerals would not precipitate on the liquidus, in accordance with the observation of Kushiro (1975).

Inasmuch as Ti^{4+} and Si^{4+} play similar roles in silicate melt structures of aluminosilicate melts, liquidus boundaries involving feldspar and pyroxene would also shift toward the pyroxene-rich portion of such systems.

Titanium concentrations in silicate melts are likely to increase during fractional crystallization until (Fe,Ti) oxides begin to precipitate. During the stage of Ti increase, stability fields of tectosilicates will expand relative to those of orthosilicates, compared with the fractionation trends in TiO_2-free systems.

This conclusion implies that fractionation trends tend toward more silica-deficient melts. Inasmuch as the liquidus relations of (Fe,Ti) oxides depend on $f(O_2)$ (*e.g.*, Osborn, 1977), the extent of these effects would depend on $f(O_2)$ even before precipitation of (Fe,Ti) oxides.

Partition coefficients of minor and trace elements between crystals and coexisting melts depend on the liquid composition (Watson, 1976, 1977; Hart and Davis, 1978; Irving, 1978; Ryerson and Hess, 1978; Mysen and Virgo, 1980b). Mysen and Virgo (1980b) found that the partition coefficients of both transition metals and rare earth elements decrease with increasing NBO/T of the melt. Inasmuch as solution of TiO_2 in melts results in a decrease in NBO/T, it would be expected that such partition coefficients would increase. No experimental data on crystal–liquid partitioning are available to test this hypothesis.

Physical properties of melts such as viscosity and density depend on both the kind of structural units present in the melt and the strength of the chemical bonds between tetrahedrally coordinated cations and bridging oxygen (Bridgman and Simon, 1953; Bockris *et al.*, 1955; Riebling, 1966; Taylor and Rindone, 1970; Bottinga and Weill, 1972). Mysen *et al.* (1980b), in a study relating melt structure to viscosity, concluded that in melts with $NBO/T \gtrsim 1$, the kind of structural units controls the melt viscosity, whereas in melts with $NBO/T < 1$, the bond strength is the controlling factor. Inasmuch as TiO_2 results in decreasing NBO/T in melts with $NBO/T > 0$, we suggest that the viscosity of such melts will increase with increasing TiO_2 content. Ti–O–Al and Ti–O–Ti bonds are probably weaker than Si–O–Al and Si–O–Si bonds because the Ti^{4+} cation is larger than that of Si^{4+}. Consequently, we suggest that solution of TiO_2 in highly polymerized aluminosilicate melts will result in a decrease in their viscosity.

Acknowledgments

Critical reviews by D. H. Eggler, P. C. Hess, I. Kushiro, C. M. Scarfe, and H. S. Yoder, Jr. are appreciated. Extensive discussions with I. Kushiro during the final stages of this research greatly improved the manuscript. This research was partly supported by NSF grant EAR 7911313 and partly by the Carnegie Institution of Washington.

References

Bando, Y. and K. Ishizuka (1979) Study of the structure of silica glass by high-resolution electron microscopy. *J. Non-Cryst. Solids, 33,* 375–382.

Bockris, J. O'M., J. D. Mackenzie and J. A. Kitchner (1955) Viscous flow in silica and binary liquid silicates. *Trans. Faraday Soc., 51,* 1734–1748.

Bottinga, Y. and D. F. Weill (1972) The viscosity of magmatic silicate liquids: a model for calculation. *Am. J. Sci., 272,* 438–475.

Brawer, S. A. (1975) Theory of vibrational spectra of some network and molecular glasses. *Phys. Rev. B, 11,* 3173–3194.

——— and W. B. White (1975) Raman spectroscopic investigation of the structure of silicate glasses. I. The binary silicate glasses. *J. Chem. Phys., 63,* 2421–2432.

——— and ——— (1977) Raman spectroscopic investigation of the structure of silicate glasses. (II) Soda–alkaline earth–alumina ternary and quaternary glasses. *J. Non-Cryst. Solids, 23,* 261–278.

Bridgman, P. W. and I. Simon (1953) Effect of very high pressure on glass. *J. Appl. Phys., 24,* 405–413.

Buddington, A. F. and D. H. Lindsley (1964) Iron-titanium oxide minerals and synthetic equivalents. *J. Petrol., 5,* 310–357.

Carmichael, I. S. E. (1967) The iron–titanium oxides of salic volcanic rocks and their associated ferromagnesian silicates. *Contrib. Mineral. Petrol., 14,* 36–65.

Chandrasekhar, H. R., M. Chandrasekhar and M. N. Manghnani (1979) Phonons in titanium-doped vitreous silica. *Solid State Commun., 31,* 329–333.

Dent Glasser, L. S. (1979) Non-existent silicates. *Z. Kristallogr., 149,* 291–305.

Etchepare, J. (1972) Study by Raman spectroscopy of crystalline and glassy diopside. In R. W. Douglas and B. Ellis, Ed., *Amorphous Materials,* p. 337–346. Wiley, New York.

Furukawa, T. and W. B. White (1979) Structure and crystallization of glasses in the $Li_2Si_2O_5$ system determined by Raman spectroscopy. *Phys. Chem. Glasses, 20,* 69–80.

——— and ——— (1980) Raman spectroscopic investigation of the structure of silicate glasses. III. Alkali-silico-germanates. *J. Chem. Phys.,* in press.

Gaskell, P. H. (1975) Construction of a model for amorphous tetrahedral materials using ordered units. *Phil. Mag., 32,* 221–229.

——— and A. B. Mistry (1979) High-resolution transmission electron microscopy of small amorphous silica particles. *Phil. Mag., 39,* 245–257.

Hart, S. E. and K. E. Davis (1978) Nickel partitioning between olivine and silicate melt. *Earth Planet. Sci. Lett., 40,* 203–220.

Irving, A. J. (1978) A review of experimental studies of crystal/liquid trace element partitioning. *Geochim. Cosmochim. Acta, 42,* 743–771.

Iwamoto, N., Y. Tsanawaki, M. Fuji and T. Hatfori (1975) Raman spectra of K_2O–SiO_2 and K_2O–SiO_2–TiO_2 glasses. *J. Non-Cryst. Solids, 18,* 303–306.

Kushiro, I. (1973) Regularities with shift of liquidus boundaries in silicate systems and their significance in magma genesis. *Carnegie Inst. Wash. Year Book, 72,* 497–502.

——— (1974) Pressure effect on the changes of the forsterite–enstatite liquidus boundary with the addition of other cations and the genesis of magmas. *Carnegie Inst. Wash. Year Book, 73,* 248–251.

——— (1975) On the nature of silicate melt and its significance in magma genesis: regularities in the shift of liquidus boundaries involving olivine, pyroxene, and silica minerals. *Am. J. Sci., 275,* 411–431.

Lazarev, A. N. (1972) *Vibrational Spectra and Structure of Silicates.* Consultants Bureau, New York.

Masson, C. R. (1977) Anionic constitution of glass-forming melts. *J. Non-Cryst. Solids, 1,* 1–42.

Mysen, B. O. and D. Virgo (1978) Influence of pressure, temperature and bulk composition on melt structures in the system $NaAlSi_2O_6$-$NaFe^{3+}Si_2O_6$. *Am. J. Sci., 278,* 1307–1322.

——— and ——— (1980a) Solubility mechanisms of carbon dioxide in silicate melts. *Am. Mineral., 65,* 885–899.

——— and ——— (1980b) Trace element partitioning and melt structure: an experimental study at 1 atm pressure. *Geochim. Cosmochim. Acta. 44,* in press.

———, F. Seifert and D. Virgo (1980a) Structure and redox equilibria of iron-bearing silicate melts. *Am. Mineral., 65,* 867–884.

———, D. Virgo and C. M. Scarfe (1980b) Relations between anionic structure and viscosity of silicate melts: a Raman spectroscopic study. *Am. Mineral., 65,* 690–710.

———, ——— and F. Seifert (1979a) Redox equilibria and melt structure in the system CaO–MgO–FeO–Fe_2O_3–SiO_2. *Carnegie Inst. Wash. Year Book, 78,* 519–526.

———, ——— and ——— (1979b) Influence of melt structure on element partitioning between olivine and melt and between clinopyroxene and melt at 1 atm. *Carnegie Inst. Wash. Year Book, 78,* 542–547.

Osborn, E. F. (1977) Origin of calc-alkali magma series of Santorini volcano type in light of recent experimental phase-equilibrium studies. *Proceedings of the International Congress on Thermal Waters, Geothermal Energy and Vulcanism in the Mediterranean Area Athens, October 1976, 3,* 154–167.

Riebling, E. F. (1966) Structure of sodium aluminosilicate melts containing at least 50 mole percent SiO_2 at 1500°C. *J. Chem. Phys., 44,* 2852–2865.

——— (1968) Structural similarities between a glass and its melt. *J. Am. Ceram. Soc., 51,* 143–149.

Ryerson, F. J. and P. C. Hess (1978) The partitioning of trace elements between immiscible silicate melts (abstr.). *EOS, 56,* 470.

——— and ——— (1980) The role of P_2O_5 in silicate melts. *Geochim. Cosmochim. Acta, 44,* 611–625.

Seifert, F., D. Virgo and B. O. Mysen (1979) Melt structures and redox equilibria in the system Na_2O–FeO–Fe_2O_3–Al_2O_3–SiO_2. *Carnegie Inst. Wash. Year Book, 78,* 511–519.

Sharma, S. K., D. Virgo and B. O Mysen (1978) Structure of glasses and melts of $Na_2O \cdot xSiO_2$ ($x = 1, 2, 3$) composition from Raman spectroscopy. *Carnegie Inst. Wash. Year Book, 77,* 649–652.

Sweet, J. R. and W. B. White (1980) Study of sodium silicate glasses and liquids by infrared spectroscopy. *Phys. Chem. Glasses, 10,* 246–251.

Taylor, M., G. E. Brown and P. H. Fenn (1980) Structure of silicate glasses. III. $NaAlSi_3O_8$ supercooled liquid at 8050°C and the effects of thermal history. *Geochim. Cosmochim. Acta,* 109–119.

Taylor, T. D. and G. E. Rindone (1970) Properties of soda aluminosilicate glasses: V. Low-temperature viscosities. *J. Am. Ceram. Soc., 53,* 692–659.

Tobin, N. C. and T. Baak (1968) Raman spectra of some low-expansion glasses. *J. Opt. Soc. Am., 58,* 1459–1460.

Verweij, H. (1979a) Raman study of the structure of alkali germanosilicate glasses. I: Sodium and potassium metagermanosilicate glasses. *J. Non-Cryst. Solids, 33,* 41–53.

——— (1979b) Raman study of the structure of alkali germanosilicate glasses. II: Lithium, sodium and potassium digermanosilicate glasses. *J. Non-Cryst. Solids, 33,* 55–69.

Virgo, D., B. O. Mysen and I. Kushiro (1980) Anionic constitution of silicate melts quenched at 1 atm from Raman spectroscopy: implications for the structure of igneous melts. *Science, 208,* 1371–1373.

———, F. Seifert and B. O. Mysen (1979) Three-dimensional network structures of glasses in the systems $CaAl_2O_4$–SiO_2, $NaAlO_2$–SiO_2, $NaFeO_2$–SiO_2, and $NaGaO_2$–SiO_2 at 1 atm. *Carnegie Inst. Wash. Year Book, 78,* 506–511.

Waff, H. S. (1977) The structural role of ferric iron in silicate melts. *Can. Mineral., 15,* 198–199.

Watson, E. B. (1976) Two-liquid partition coefficients: experimental data and geochemical implications. *Contrib. Mineral. Petrol., 56,* 119–134.

——— (1977) Partitioning of manganese between forsterite and silicate liquid. *Geochim. Cosmochim. Acta, 41,* 1363–1374.

Manuscript received, November 15, 1979;
accepted for publication, May 28, 1980.